J. Am. Chem. Soc. 1993, 115, 647–652

Molecular Dynamics Study of Methane Hydration and Methane Association in a Polarizable Water Phase

Daniel van Belle* and Shoshana J. Wodak

Contribution from the Unité de Conformation des Macromolécules Biologiques, Université Libre de Bruxelles, Av. P. Héger, CP 160/16, B-1050 Bruxelles, Belgium. *Received May 1, 1992*

Abstract: Molecular dynamics simulations are used to investigate the influence of adding an explicit polarization term to the water potential on the structural and dynamic properties of aqueous methane solutions and on methane–methane association in water. Calculations are performed using respectively two different water models: the three-center polarizable water model (PSPC), where the many-body effects are treated explicitly using the extended Lagrangian method, and the mean-field classical SPC model. Comparing the results obtained from the two sets of calculations we find that electronic polarization of the water molecules has a subtle though significant influence on the structure and dynamics of water molecules surrounding the hydrophobic solute. But its most remarkable influence by far is on the methane–methane potential of mean force: addition of the polarization term to the water potential effectively abolishes the much questioned solvent-separated minimum found in many previous studies with nonpolarizable water models. Polarizable water models thus appear to yield an improved physical picture of the system and should be well suited for investigating the process of hydrophobic association.

I. Introduction

The thermodynamics of transferring apolar species from the ideal gas phase to aqueous solution are characterized, at room temperature, by a small negative change in enthalpy and a large negative change in entropy, leading to an overall positive free energy of hydration.[1] The classical picture of the hydrophobic effect ascribes the negative change in entropy to the increased structure of water around the solute and consequently to a loss of entropy.[2] The tendency of apolar solutes to associate in water, commonly termed hydrophobic interaction, is then explained by the requirement to reduce the total surface area in contact with the water molecules.[2]

Dilute aqueous solutions of simple nonpolar solutes such as simple alkanes and noble gases can be considered as the prototype of hydrated hydrophobic systems, and their analysis has therefore attracted much interest. Manifestations of the hydrophobic effect are difficult to measure in such solutions owing to the low solubility of apolar species in water. Computer simulations, on the other hand, are able to provide a detailed microscopic description of such systems and are hence extremely valuable in providing insight into the physical factors that are at play. An extensive body of theoretical work is available on systems such as methane in water. Most of it focuses on studies of water structure around the hydrophobic species.[3–11] More recently, increased availability of computer power made it possible to compute solvation free energies of these systems and investigate individual energetic components.[12–15]

Computer simulations have also been used to investigate hydrophobic interaction. The study by Geiger and co-workers[16] of two hydrophobic particles in water was the first to detect two stable configurations for this system. One, where the apolar particles make van der Waals contacts, and a second configuration, where these particles are separated, on the average, by one water molecule. This quite unexpected and counterintuitive result has since then been confirmed by many other theoretical studies using different methodologies.[17–23] In these studies, Monte Carlo and molecular dynamics techniques were used to compute the potential of mean force (pmf) between two apolar particles in water. This potential being expressed as the reversible work required to bring the two molecules from infinite separation to a distance r revealed the existence of at least one minimum in addition to that where the two apolar molecules are in contact. Pratt and Chandler[24] have reached similar conclusions for the case of two hard spheres in water using the integral equations formalism together with the experimental pair correlation function of pure water.

Notwithstanding the consensus reached by the theoretical investigations, the existence of the water-separated state has long been a subject of debate, as the reasons underlying its formation have remained unclear.

Aqueous solutions of small apolar compounds are, despite their simplicity, rather tricky systems to simulate, and properties computed from simulations of such systems tend to be rather sensitive to details in the parametrization of the water–water interaction potential.[3] Having a satisfactory representation of pure liquid water is therefore paramount for the accurate description of these simple solvated systems. Explicit treatment of electronic polarization effects,[25–32] as opposed to the more common practice

---

(1) Ben-Naim, A.; Marcus, Y. *J. Chem. Phys.* **1984**, *81*, 2016.

(2) Frank, H. S.; Evans, W. *J. Chem. Phys.* **1945**, *13*, 507.

(3) Owicki, J. C.; Scheraga, H. A. *J. Am. Chem. Soc.* **1977**, *99*, 7413.

(4) Swaminathan, S.; Harisson, S. W.; Beveridge, D. L. *J. Am. Chem. Soc.* **1978**, *100*, 5705.

(5) Rossky, P. J.; Karplus, M. *J. Am. Chem. Soc.* **1978**, *101*, 1913.

(6) Pangali, C.; Rao, M.; Berne, B. J. *J. Chem. Phys.* **1979**, *71*, 2982.

(7) Rapaport, D. C.; Scheraga, H. A. *J. Phys. Chem.* **1982**, *86*, 873.

(8) Okazaki, S.; Nakanishi, K.; Touhara, H.; Watanabe, N. *J. Chem. Phys.* **1981**, *74*, 5863.

(9) Bolis, G.; Clementi, E. *Chem. Phys. Lett.* **1981**, *82*, 147.

(10) Swope, W. C.; Andersen, H. C. *J. Phys. Chem.* **1984**, *88*, 6548.

(11) Laaksonen, A.; Stilbs, P. *Mol. Phys.* **1991**, *74*, 747.

(12) Postma, J. P. M.; Berendsen, H. J. C.; Haak, J. R. *Faraday Symp. Chem. Soc.* **1982**, *17*, 55.

(13) Straatsma, T. P.; Berendsen, H. J. C.; Postma, J. P. M. *J. Chem. Phys.* **1986**, *85*, 6720.

(14) Jorgensen, W. L.; Blake, J. F.; Buckner, J. K. *Chem. Phys.* **1989**, *129*, 193.

(15) Guillot, B.; Guissani, Y.; Bratos, S. *J. Chem. Phys.* **1991**, *95*, 3643.

(16) Geiger, A.; Rahman, A.; Stillinger, F. H. *J. Chem. Phys.* **1979**, *70*, 263.

(17) Pangali, C.; Rao, M.; Berne, B. J. *J. Chem. Phys.* **1979**, *71*, 2975.

(18) Rapaport, D. C.; Scheraga, H. A. *J. Phys. Chem.* **1982**, *86*, 873.

(19) Ravishanker, G.; Mezei, M.; Beveridge, D. L. *Faraday Symp. Chem. Soc.* **1982**, *17*, 79.

(20) Ravishanker, G.; Beveridge, D. L. *J. Am. Chem. Soc.* **1985**, *107*, 2565.

(21) Zichi, D. A.; Rossky, P. J. *J. Chem. Phys.* **1985**, *83*, 797.

(22) Watanabe, K.; Andersen, H. C. *J. Am. Chem. Soc.* **1986**, *90*, 795.

(23) Jorgensen, W. L.; Buckner, J. K.; Boudon, S.; Tirado-Rives, J. *J. Chem. Phys.* **1988**, *89*, 3742.

(24) Pratt, L. R.; Chandler, D. *J. Chem. Phys.* **1977**, *67*, 3683.

(25) Rullman, J. A. C.; van Duijnen, P. Th. *Mol. Phys.* **1988**, *63*, 451.

(26) Sprik, M.; Klein, M. L. *J. Chem. Phys.* **1988**, *89*, 7556.

(27) van Belle, D.; Froeyen, M.; Lippens, G.; Wodak, S. J. *Mol. Phys.*, in press.

(28) Ahlström, P.; Wallqvist, A.; Engström, S.; Jönsson, B. *Mol. Phys.* **1989**, *68*, 563.

(29) Pearlman, D. A.; Kollman, P. A. *J. Chem. Phys.* **1989**, *91*, 7831.

(30) Sprik, M.; Klein, M. L.; Watanabe, K. *J. Phys. Chem.* **1990**, *94*, 6483.

(31) Sprik, M. *J. Phys. Chem.* **1991**, *95*, 2283.

0002-7863/93/1515-647\$04.00/0

of incorporating them in an average way, constitutes a welcome refinement of the water–water interaction potential. These effects strongly depend on the local environment of the water molecules and may therefore be modulated in a nontrivial way by the presence of the hydrophobic solute. This could in turn significantly influence structural and dynamic properties of the water molecules surrounding the solute and consequently bear on the physics of the hydrophobic effect. Except for a study of polarizable water in the presence of a hydrophobic wall,[32] these issues have not been previously investigated by simulation methods.

The present study uses molecular dynamics simulations to investigate the influence of adding an explicit polarization term to the water potential on the structural and dynamic properties of aqueous solutions containing one and two methane molecules and on the potential of mean force between two methanes dissolved in water. To this end, the same calculations are performed using two different force fields for the water phase. In one, the three-center polarizable water model (PSPC)[28] is used, and many-body electronic polarization effects are incorporated explicitly by the extended Lagrangian method previously described.[26,27,33] In the other, the solvent is represented by a pairwise additive force field using the classical SPC model.[34] A comparative analysis of results obtained from the two sets of calculations shows that electronic polarization of the water molecules has a subtle though significant influence on the microscopic description of hydrophobic hydration and, more importantly, that it has a marked effect on the microscopic description of hydrophobic association.

II. Methods and Computational Procedure

II.1 Treatment of Electronic Polarization. Assuming a scalar polarizability and linear polarization, the induced dipole moment of the *k*th water molecule is expressed as

$$\mathbf{p}_k = \alpha_k \mathbf{E}_k \tag{1}$$

where α_k is the polarizability of the *k*th PSPC water molecule[28] (1.44 Å^3) and $\mathbf{E}_k$ is the total electric field measured at the oxygen nucleus of that molecule.

The induced polarization is computed using an approach recently described in detail.[26,27] Only its main features are therefore presented here.

To compute the induced polarization, the dipole moment $\mathbf{p}_k$ is treated as an additional (internal) degree of freedom of the water molecule. Using the extended Lagrangian formalism,[33] the system is represented in a new phase space defined by the Cartesian coordinates of each water molecule, the induced dipole associated with it, and the conjugated momenta of both. The methane molecule is considered as nonpolarizable. Thus, for each extra degree of freedom *k*, we add to the Lagrangian of the system a potential energy term.[35] This term contains two contributions, the energy of the induced dipole given an external electric field and the energy for creating the induced dipole. The extra degrees of freedom also have a kinetic energy term, $K_p = 1/2\sum_k m_p \dot{p}_k{}^2$, associated with them, where $\dot{p}_k$ is the time derivative of the induced dipole and m_p is an "inertial factor" associated with the extra dynamical variables whose dimensions are those of a mass·charge^{-2}. With the standard procedure of Lagrangian mechanics, the following equation of motion is then derived:

$$m_p \ddot{\mathbf{p}}_k = \mathbf{E}_k - \frac{\mathbf{p}_k}{\alpha_k} \tag{2}$$

where $\ddot{\mathbf{p}}_k$ is the second time derivative of the induced dipole. Integration of eq 2, which is readily performed by standard numerical integration algorithms such that of Verlet,[36] yields the value of $\mathbf{p}_k$, which is then used to compute the electrostatic energy terms and the forces that depend on the induced dipoles. The dipole inertial factor determines the response time scale of the dipoles to fluctuations of the electric field produced by the motion of the particles. A fixed value of 0.5 g/|e|^2 is used based on a detailed comparison of the static properties of pure PSPC liquid water with the full iterative scheme for solving eq 1.[27]

This procedure for computing the many-body polarization effects is extremely efficient, with an increase of no more than a factor of 2 in computer time, essentially due to the overhead associated with computing energies and forces between dipoles.

II.2 Potential of Mean Force (pmf) Calculation. The free energy profile as a function of the intermolecular distance between two methane molecules can be calculated using the free energy difference perturbation technique which leads to[37,38]

$$\Delta A(r \rightarrow r + \Delta r) = -k_b T \ln \langle e^{-\Delta U / k_b T} \rangle r \tag{3}$$

where the angle brackets with subscript *r* represent an ensemble average with the intermolecular distance between the two methanes held fixed at distance *r*; ΔU is the potential energy difference obtained by changing the intermolecular distance from *r* to $r + \Delta r$.

In performing such computations it is important to evaluate the associated uncertainty. This is done in the following manner. The configuration ensemble computed at a given distance *r* is broken up into blocks, each containing *n* configurations.[39] Values of ΔA are then computed using ensemble averages obtained on individual blocks. This yields ν independent ΔA evaluations, with ν corresponding to the number combinations of individual blocks used in the computation. This serves as a statistical distribution, from which a standard error σ is computed, using as a reference value the free energy calculated from all the configurations in the trajectory for each *r* value. Since ν varies with block length *n*, a series of σ values is obtained. The representative σ value of the solvation free energy is then taken as that which remains relatively *constant* within a range of block lengths, *n*. The errors at individual distance points are added up in order to obtain the total uncertainty over the entire path.

II.3 Simulation Conditions. The first set of simulated systems, labeled system I, consists of 215 water molecules at a density of 1 g/cm^3 plus 1 methane molecule. The second set, labeled system II, consists of 341 water molecules at the same density, plus 2 methanes held fixed at their contact distance of 4 Å. The methane interacts with the water molecules through a single Lennard–Jones potential and is taken as nonpolarizable, following previous studies of an equivalent system.[40] The energy parameters for the methane–water interaction potential are obtained by the conventional Lorentz–Berthelot combination rules. We thus obtain $\sigma_{\mathrm{MW}} = 3.448$ Å and $\epsilon_{\mathrm{MW}} = -0.214$ kcal/mol for the classical SPC system and $\sigma_{\mathrm{MW}} = 3.497$ Å and $\epsilon_{\mathrm{MW}} = -0.195$ kcal/mol for the polarizable PSPC system.

A site–site spherical cutoff at 8.5 Å is applied to all the terms in the potential; the water–water electrostatic potential term is multiplied over the entire distance range between 0 and the cutoff distance by the termination function[41,42] $S(r) = (1 - (r/r_c))^2$ where *r* is the distance between two charged sites and r_c is the cutoff distance. In the case of the polarizable system, the electric field arising from permanent charges is modified in the same way. A time step of 2×10^{-15} s is used throughout.

The molecular dynamics simulations have been performed in the isovolumic–isothermal *N, V, T* ensemble; this ensemble is sampled by the extended Lagrangian Nosé method,[33] with the temperature set to 300 K.

---

[32] Wallqvist, A. *Chem. Phys. Lett.* **1990**, *165*, 437.

[33] Nosé, S. *Mol. Phys.* **1984**, *52*, 255.

[34] Berendsen, H. J. C.; Postma, J. P. M.; van Gunsteren, W. F.; Hermans, J. In *Intermolecular Forces*; Pullman, B., Ed.; Dordrecht, 1981; p 331.

[35] Böttcher, C. J. F. *Theory of Electric Polarisation*, 2nd ed.; Elsevier Publishing Company: Amsterdam, 1973.

[36] Verlet, L. *Phys. Rev.* **1967**, *159*, 98.

[37] McQuarrie, D. A. *Statistical Mechanics*; Harper and Row: New York, NY, 1976.

[38] Tobias, D. J.; Brooks, C. L., III. *Chem. Phys. Lett.* **1987**, *142*, 472.

[39] Allen, M. P.; Tildesley, D. J. *Computer Simulation of Liquids*; Oxford University Press: Oxford, 1986; p 191 and references therein.

[40] Jorgensen, W. L.; Madura, J. D.; Swenson, C. J. *J. Am. Chem. Soc.* **1984**, *106*, 6638.

[41] Pettitt, B. M.; Rossky, P. J. *J. Chem. Phys.* **1982**, *77*, 1451.

[42] Prévost, M.; van Belle, D.; Lippens, G. Wodak, S. J. *Mol. Phys.* **1990**, *71*, 587.

The pressures measured from the virial of forces in the mean-field SPC and in the polarizable PSPC systems were the same within the statistical accuracy (~800 ± 100 atm).

The equations of motion of the particles as well as the equations of motion associated with the extra variables are integrated in Cartesian space with the use of the velocity version[43] of the algorithm of Verlet. The internal degrees of freedom of the water molecules are constrained using the RATTLE[43] method. The general molecular dynamics procedure described above is implemented in the BRUGEL[44] package.

To compute the potential of mean force between two methanes dissolved in water a total trajectory of 670 ps was generated for system II. This trajectory consisted of 17 individual molecular dynamics runs, each performed at a given methane–methane separation distance *r*, with *r* varying from 8.0 to 3.75 Å, in steps of 0.250 Å. Each run consisted of 10 ps of equilibrium followed by 20 ps to calculate the averages. In order to improve convergence, in the distance interval of 7.0–5.25 Å the trajectories used for averaging were extended to 40 ps. At the methane–methane distance of 4 Å, an additional 60 ps of molecular dynamics simulations have been performed for the purpose of computing the average properties of system II.

III. Results and Discussion

III.1 Influence of Electronic Polarization of Water on Methane Hydration. To determine the influence of including an explicit electronic polarization term in the water potential on the hydration properties of the methane solutions, static and dynamic properties of the water surrounding the nonpolar solute have been investigated in trajectories generated with and without this term included.

III.1.1 Static Properties. The methane–water radial distribution functions (rdf's) computed from simulations with the mean-field SPC and the polarizable PSPC models are shown in Figure 1a and 1b for systems I (single methane in water) and II (methane "dimer" at 4.0-Å separation), respectively. These figures also display the distance dependence of the coordination number computed from the corresponding rdf's.

In both systems, the methane–water functions display appreciable structure with two maxima at approximately 3.7 and 6.5 Å. The positions of these maxima are at slightly larger distances for the polarizable water model, consistent with the larger methane–water Lennard-Jones σ_{MW} parameter (0.05 Å) associated with this model. The height of the first peak with the PSPC model exceeds that with SPC for system I (Figure 1a). This yields 4.8 neighbors (at 3.7 Å) and 3.5 neighbors (at 3.6 Å) for PSPC and SPC, respectively, indicating that in this system the PSPC water around the methane is somewhat more structured than its mean-field equivalent. In system II on the other hand, the height of the first peak is almost identical for both water models (Figure 1b), but it is significantly lower than that in system I, reflecting the fact that individual methanes in the "dimer" are not completely surrounded by water. The corresponding number of neighbors is 3 (at 3.7 Å) for both water models. Further subtle differences appear at larger distances and are described in the legend of Figure 1.

The water–water rdf's averaged over all the molecules in the system were also computed and found to be identical to those calculated from simulations of pure water[27,28] (results not shown), indicating that, overall, the solvent structure is not perturbed by the presence of the hydrophobic solutes considered in this study.

These results show that structural properties of the water phase in our mixture are well represented by our simulation procedures both with the permanent SPC and polarizable PSPC models. Similar conclusions were reached in a previous study of pure liquid water.[27,28]

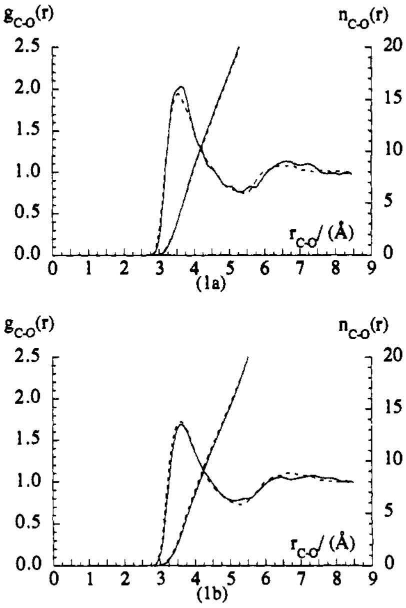

Figure 1. Methane–oxygen pair correlation functions and corresponding coordination numbers. Data for the polarizable PSPC system are given by full lines, those for the mean-field SPC system are given by dashed lines. (a) System I, 215 water molecules plus 1 methane. In this system, integration to the point where the radial distribution function crosses the unity value following the first peak (4.6 Å) yields about 15 neighbors in both water models. At larger distances, i.e., corresponding to the minimum at 5.3 Å, it yields 20 neighbors for the polarizable model and 21 neighbors at 5.4 Å for the permanent one. This difference may not be significant because the number of neighbors tends to increase sharply at large distances where the positions of the minima are ill-defined due to poor statistics (±0.07 error at the first maximum of the rdf) even though they are computed from rather long trajectories (50 ps). (b) System II, 341 water molecules plus 2 methanes held fixed at an intermolecular distance of 4 Å. In this system the permanent SPC model displays more structure than PSPC (the minimum is deeper, and the second maximum is higher and better defined). It also appears that the second peak of the PSPC system "splits" into two peaks, this tendency being already visible in the PSPC rdf of system I. Integrating the rdf out to the point where it crosses unity yields 11 neighbors for both models, while integration out to the minimum yields 16 neighbors at 5.1 Å and 18 neighbors at 5.3 Å for the polarizable and permanent systems, respectively. Again, the differences at long distances are probably not significant due to the fact that the minimum in the rdf of the polarizable system is very flat. Note that the computed uncertainties are somewhat smaller in system II since the rdf are calculated on two methanes (±0.05 at the first maximum).

In addition to structural properties, we also analyze the magnitude of the induced water dipoles around the apolar solute. Our results show that water molecules in contact with the hydrophobic species are less polarized than their counterparts in the bulk. The average drop in polarization magnitude is 8% at 3.0 Å, 2% at 3.5 Å, and 1% at 4 Å for system I. In system II, the change in polarization magnitude is somewhat larger, it is 10% at 3.0 Å, 6% at 3.5 Å, and 4% at 4 Å. This is well understood since the presence of the apolar solute tends to lower the local density of polarizing dipoles. This effect is however limited to the neighborhood of the methane and is completely damped at distances of about 5 Å after the first peak of the solute–solvent pair correlation function. A much more significant drop in the magnitude of induced water dipoles, 25%, has been computed for water molecules near a hydrophobic wall.[32] The trend observed in the drop of polarization magnitude in the methane dimer and monomer systems confirms that the influence of the hydrophobic solute on the water dipole moment depends on the size of the solute.

The average angle between the induced and the permanent dipole components also shows a change due to the presence of the apolar solute. The induced dipole is less parallel to the permanent dipole at 3 Å from the solute center (24° ± 0.3°) than at 5 Å (21° ± 0.3°).

The total dipole of the polarizable water molecule, calculated as the vectorial sum of the induced and permanent dipoles, amounts to 2.7 D at 3.0 Å from the solute and relaxes to 2.8 D in the bulk. This corresponds to a loss of about 4–5% at the contact

---

(43) Swope, W. C.; Andersen, H. C.; Berens, P. H.; Wilson, K. R. *J. Chem. Phys.* **1982**, *76*, 637.

(44) Delhaise, P.; van Belle, D.; Bardiaux, M.; Alard, P.; Hamers, P.; van Cutsem, E.; Wodak, S. *J. Mol. Graphics* **1985**, *3*, 116.

Table I. Self-Diffusion Coefficients and Reorientational Times of Water in the First Solvation Shell of Methane(s)

	SPC (II)[a]	SPC (I)[b]	SPC*[c]	PSPC (II)[a]	PSPC (I)[b]	PSPC*[c]
D (10^{-9} m^2/s)	2.9 ± 0.4	3.2 ± 0.6	4.6 ± 0.2	2.0 ± 0.4	2.2 ± 0.3	2.4 ± 0.2
$\tau_\alpha^{(1)}$[d] (ps)	5.6 ± 0.8	2.9 ± 0.6	2.4 ± 0.1	6.4 ± 0.9	5.2 ± 0.8	4.8 ± 0.3
$\tau_\beta^{(1)}$[d] (ps)	3.0 ± 0.8	2.0 ± 0.6	1.6 ± 0.1	2.9 ± 0.8	2.6 ± 0.5	2.3 ± 0.2
$\tau_\gamma^{(1)}$[d] (ps)	4.2 ± 0.6	2.5 ± 0.5	2.4 ± 0.1	3.1 ± 0.5	3.1 ± 0.4	3.2 ± 0.2

[a] (II) refers to system II, 341 water molecules plus 2 methanes, the intermolecular distance being held fixed at 4.0 Å. [b] (I) refers to system I, 215 water molecules plus 1 methane. [c] The asterisk denotes pure liquid values. [d] Indices α, β, γ correspond to the molecular axes as defined in Figure 3; index (1) refers to the first-order Legendre polynomial.

distance with the hydrophobic solute(s). When averaged over all water molecules in the system, the magnitude of the induced dipoles as well as the angle between the induced and permanent dipoles is exactly the same in the methane solution studied here as in the pure liquid.[27]

To investigate the consequences of this loss of polarization on structural properties we compute the water–water rdf's for water molecules in the first solvation shell of the methanes in the monomer and dimer (a water molecule is considered to belong to this shell if its distance to the methane is less than 4.5 Å). Figure 2a and 2b displays these functions obtained with the mean-field SPC and polarizable PSPC models, in systems I and II respectively.

We see first of all that in both systems the first peaks of the water–water rdf's are lower than that of the bulk water rdf, a direct consequence of the loss of water neighbors due to contact with the hydrophobic solute.

There are, however, distinct differences between the rdf's of SPC and PSPC, which may be more physically relevant. In system I the drop of the first peak is more pronounced with SPC than with PSPC. In system II, the first peak drops further in the polarizable model while the corresponding peak of the permanent model remains unchanged (Figure 2 insets). These latter findings are consistent with the more pronounced loss of polarization that we observe for the PSPC water molecules in the first solvation shell of system II relative to system I. They agree indeed with conclusions of earlier studies on the influence of the electrostatic part of the potential on the shape of the pair correlation function of pure water, in particular, that weakening the electrostatic interactions will decrease the height of the first peak in the oxygen–oxygen rdf.[41,42]

The difference we observe between the rdf's of SPC and PSPC in system I is on the other hand somewhat counterintuitive, considering that here, too, first shell PSPC waters lose polarization relative to bulk water, while SPC waters do not. A possible explanation could be that the small size of the nonpolar solute in system I represents a limiting case where the loss of polarization in first shell waters is small enough to be overridden by the ability of their dipoles to reorient through induction effects so as to optimize interactions with neighboring water molecules without adjustment of atomic positions.

This could also be the cause of the increased structure of the PSPC water around the methane as compared to SPC in system I (Figure 1a). Furthermore, the fact that, in system II, the first peak of the methane–water rdf drops to the same level for both water models (Figure 1b) shows that relative to its height in system I, this peak has decreased more in the polarizable model than in its mean-field equivalent. This is once again consistent with a further weakening of the electrostatic interactions in PSPC, upon going from a single methane to two molecules. We would expect these effects to be amplified in larger hydrophobic solutes and, possibly, to depend also on their surface curvature.

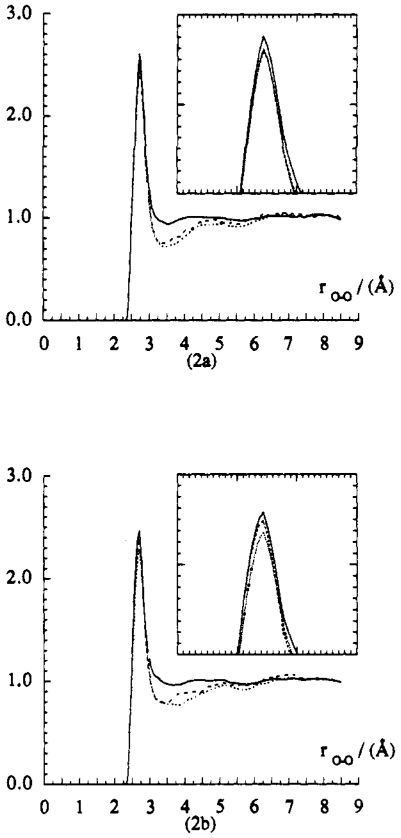

(2a)

(2b)

Figure 2. Oxygen–oxygen pair correlation function in the first solvation shell of the hydrophobic solute. The central water molecule is taken to be within 4 Å of the methane. (a) Mean-field SPC system, (b) polarizable PSPC system. Plain curve: pure liquid water. Dashed curve: system I. Dotted curve: system II.

III.1.2. Dynamic Properties: Diffusion and Reorientational Times. Because the effect of the hydrophobic solute is greatest for the water molecules which are in its immediate vicinity, we focus the analysis on the first solvation shell. Here, a water molecule is considered to belong to this shell if it is within a radius r from the center of the methane and has not left this perimeter during the simulation for a continuous period longer than 10% of a maximum correlation time s. In all cases r is fixed to 4 Å and s to 4 ps. The translational diffusion coefficient D is evaluated from the mean square displacement correlation function.[45] The orientational properties are studied by calculating the first-order Legendre polynomial of the orientation vectors (Figure 3):

$$\langle P_1(\mathbf{e}^x(t)\cdot\mathbf{e}^x(0))\rangle = \langle \mathbf{e}^x(t)\cdot\mathbf{e}^x(0)\rangle \qquad (4)$$

where $\mathbf{e}^x$ are unit vectors defined in the molecular reference frame α, β, γ.

The characteristic times $\tau_x^{(1)}$ are calculated by a least square fit, assuming an exponential decay for the reorientation functions defined by eq 4. The short times (up to 0.5 ps), corresponding to the librational motion of the water molecule in its neighbors cage, were not included in the fit.

The translational diffusion coefficients D and the orientational correlation times in the molecular frame α, β, γ, calculated for systems I and II, are listed in Table I. The pure liquid water values are provided for comparison.[27,42] The given uncertainties are the standard errors calculated by breaking up the total trajectory into blocks of 10 ps each.

We see that overall, the presence of methane tends to slow down the dynamical properties, in agreement with the well-known "freezing effect" of the hydrophobic solutes on the surrounding water molecules.[2] This effect is somewhat more pronounced in the SPC system than with PSPC, possibly due to the smaller

---

(45) Hansen, J. P.; McDonald, I. R. *Theory of Simple Liquids*; Academic Press: London, 1987.

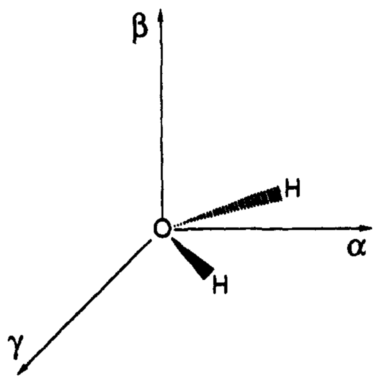

Figure 3. Definition of the coordinate system used to describe the reorientational motion. α is the vector along the permanent dipole moment or the in-plane component. β is the out-of-plane vector, normal to the molecular plane defined by the position of the oxygen and the positions of the two hydrogen atoms. γ is defined along the hydrogen–hydrogen relative vector.

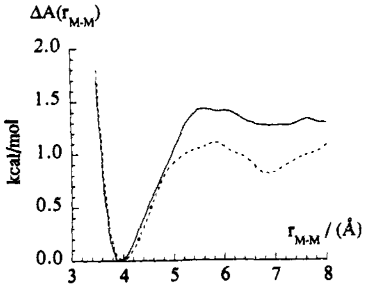

Figure 4. Potential of mean force of two methanes in water as a function of the intermolecular distance. Plain curve: mean-field SPC system. Dotted curve: polarizable PSPC system.

induced dipoles of the PSPC water molecules in contact with the methane, resulting in weaker mutual interactions and forces. This will in turn increase the diffusion coefficient and accelerate the reorientation of the molecules, counterbalancing somewhat the freezing effect. Furthermore, the decrease of the transport properties is more pronounced in system II (with two methanes) than in system I (with one methane) (Table I), indicating a clear influence of the size of the hydrophobic solute. A comparative study with different hydrophobic solute sizes and shapes should thus be of interest.

It is noteworthy that the dynamical properties calculated, considering all the water molecules in our systems using PSPC (extended Lagrangian method) and SPC, respectively, are identical to those obtained previously for pure water using the corresponding water models.[27,42] In both cases, PSPC is seen to yield results closer to the experimental measures.

III.2 Influence of Electronic Polarization of Water on Methane Association. Having shown that adding an explicit electronic polarization term in the water potential has a subtle yet significant influence on methane hydration properties, we investigated the effect of this term on the association of methane in water by computing the methane–methane potential of mean force (pmf).

The pmf's computed as a function of the inter-methane distance for the SPC and PSPC systems, respectively, are shown in Figure 4, where the 0 energy level is taken to be the minimum of each curve. The statistical uncertainty for each point relative to the adjacent points ranges from 0.01 to 0.1 kcal/mol, depending on the free energy difference itself. The total uncertainty on both ends of the curve amounts to 0.1–0.35 kcal/mol.

We see that for both water models, the minima occur at 4 Å, corresponding to the methane–methane contact distance. This near perfect coincidence is the consequence of the methane–methane energy parameters being the same in both systems. At larger intermolecular distances, however, the curves display quite a different shape. The height of the energy barrier for separating the methanes is 1.5 kcal/mol in the polarizable PSPC system but only 1.0 kcal/mol in the permanent SPC system. Furthermore, the permanent model displays a well-defined minimum at 6.9 Å corresponding to the solvent-separated configuration. This distance corresponds to a linear arrangement between the centers of the two methanes and that of an intervening water molecule, as illustrated in Figure 5. The energy barrier to squeeze this water molecule out is 0.35 kcal/mol. In the polarizable system, this second minimum is very ill-defined, the height of the barrier being reduced to only 0.15 kcal/mol. The fact that the water molecule situated between the two methanes has a smaller induced dipole can qualitatively explain this difference.

The results we obtain with the permanent water model are in very good agreement with those obtained by other authors.[17,22,40] Although, relative to the results of Jorgensen et al.,[23] the position of the minimum corresponding to the solvent-separated configuration is shifted to larger distances in our calculations, probably due to differences in the water models used.

The raised energy barrier for separating the two methanes in the polarizable system could be explained by the traditional view of the hydrophobic effect, which considers differences in hydration properties between the aggregated and nonaggregated species. Indeed, we have shown above that the number of water neighbors of the isolated methane is larger in the polarizable model than in the permanent one while the number of neighbors of the dimer in contact is equal in both models. We can thus deduce that the polarizable system, relative to the permanent model, releases more water molecules to the bulk when the two methanes associate.

The polarizable water system is thus likely to promote aggregation of hydrophobic species in water through the subtle influence that electronic polarizability exerts on their hydration properties. In general, there will be aggregation of hydrophobic particles if the probability to meet a third particle (a diffusion-controlled process) is larger than the probability to dissociate the complex of two molecules and so on. We see that the polarizable model lowers the probability for the complex to dissociate and raises the energy level of the solvent-separated configuration, while at the same time decreasing the energy barrier of squeezing out the water molecule from the solvent-separated configuration, a net effect that should favor aggregation relative to the permanent model.

IV. Conclusions

Incorporation of electronic polarization of the water molecules in computer simulations is shown to have perceptible effects on the hydration properties of methanes and a marked effect on methane association in water.

Polarizable water molecules around the hydrophobic solute experience a loss in their dipole moment. This results in weaker electrostatic interactions with neighboring molecules and hence

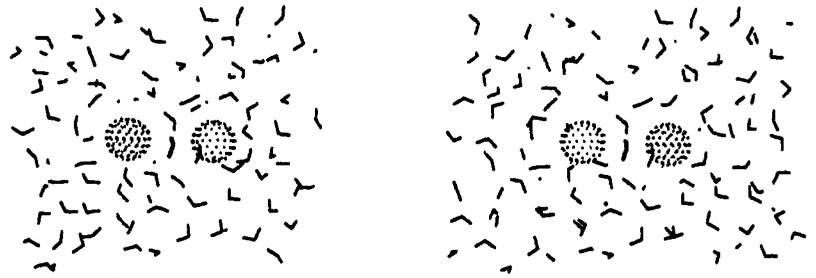

Figure 5. A typical solvent-separated configuration in simulations with SPC, with the methane–methane distance at 6.9 Å. In this configuration a water molecule (bold) is located between the two methanes.

less structure than in the bulk. These effects are essentially limited to the first solvation shell but increase in magnitude with the size of the hydrophobic solute. Loss of structure relative to bulk is also observed in the nonpolarizable water around the solute, but dependence on solute size is absent.

In accord with previous findings we see that the major influence on the nonpolar solute on the water phase is to slow down the motion of the waters surrounding it; the effect to which the important unfavorable entropic contributions to hydrophobic solvation have been attributed.[2]

Due to the weakened electrostatic interactions, polarizable water surrounding the solute, being able to reorient faster than nonpolarizable water, will have its motion less affected. It is suggested that here too the size and possibly shape of the nonpolar solute would influence the magnitude of the decrease for the polarizable water but not for the mean-field one.

In line with the results reported here on the subtle influence of electronic polarization on the structural properties of water surrounding a single methane, we find that molecular dynamics simulations with both water models yield very similar values for the methane hydration free energies, which are furthermore in good agreement with the experimental measures (results to be presented elsewhere).

The most remarkable outcome of this study concerns the striking influence of including electronic polarization effects for water on the computed methane–methane potential of mean force. The energy barrier to separate the two methanes is higher, while that for squeezing out the water from the solvent-separated configuration is lower, nearly abolishing the minimum corresponding to the solvent-separated configuration. The latter has been reproduced by a large number of previous studies, all using noninducible water models, but was regarded by many as counterintuitive. The present results and the recent findings that polarizable models also yield a more realistic representation of pure water diffusion properties[27,28] suggest that including electronic polarization in water simulations yields an improved physical description of the system, and should be instrumental in future studies of hydrophobic association in water.

Registry No. H_2O, 7732-18-5; CH_4, 74-82-8.

Theoretical Studies of Elimination Reactions. 3. Gas-Phase Reactions of F^- with $(CH_3)_2CHCl$ and $CH_3CH_2CH_2Cl$. The Effect of Methyl Substituents

Scott Gronert

Contribution from the Department of Chemistry and Biochemistry, San Francisco State University, San Francisco, California 94132. Received June 17, 1992

Abstract: The effect of methyl substitution on E2 and S_N2 mechanisms was evaluated by applying high-level ab initio calculations to the gas-phase reactions of F^- with $(CH_3)_2CHCl$ and $CH_3CH_2CH_2Cl$. E2 (anti and syn) as well as S_N2 pathways were investigated, and transition states were located at the 6-31+G* level. The nature of all stationary points was confirmed with analytical frequencies. Energy comparisons were made at the MP2/6-31+G**//HF/6-31+G* level, corrected for zero-point vibrations (scaled by 0.9). As expected, the addition of a methyl group at the α-carbon increases the S_N2 barrier (by 2.2 kcal/mol); however, in the proper conformation, a methyl group at the β-carbon reduces the barrier (by 1.7 kcal/mol). Methyl groups at either carbon stabilize the E2 transition states by about 2–3 kcal/mol. Both systems have a strong stereochemical preference ($\sim$13 kcal/mol) for anti rather than syn eliminations. The E2(anti) transition states are periplanar, and their geometries suggest a synchronous E2 elimination. The E2(syn) reactions are more E1cb-like and involve syn clinal rather than syn periplanar transition states. The $FH_\beta–C_\beta–C_\alpha–Cl$ dihedral is $\sim 35°$. In the syn transition states, the barrier to rotation around the $C_\alpha–C_\beta$ bond is small and the transition-state energy varies little for dihedral angles between 0 and 60° (1–3 kcal/mol). A review of past theoretical work indicates that syn clinal rather than syn periplanar conformations may be generally preferred for gas-phase syn eliminations. A comparison of the energetics of the S_N2 and E2 reactions predicts that elimination will dominate in the propyl systems.

Introduction

The S_N2 substitution and E2 elimination reactions have played fundamental roles in the development of modern physical organic chemistry.[1-4] During the past 50 years, there have been countless reports on the kinetics and selectivities of these reactions. On the basis of this work, detailed mechanisms have been formulated and generalizations have been developed concerning the effects of substituents. In fact, substituent effects have played a pivotal role in characterizing the mechanisms and transition states of S_N2 and E2 reactions. Although it is clear that the S_N2 reaction simply

---

(1) For E2 reactions, see: (a) Bartsch, R. A.; Zavada, J. *Chem. Rev.* **1980**, *80*, 454. (b) Bartsch, R. A. *Acc. Chem. Res.* **1975**, *8*, 128. (c) Ingold, C. K. *Structure and Mechanism in Organic Chemistry*, 2nd ed.; Cornell University Press: Ithaca, NY, 1969. (d) Saunders, W. H., Jr.; Cockerill, A. F. *Mechanism of Elimination Reactions*; Wiley Interscience: New York, 1973; Chapter 1. (e) Saunders, W. H., Jr. *Acc. Chem. Res.* **1976**, *9*, 19. (f) Saunders, W. H., Jr. In *The Chemistry of Alkenes*; Patai, S., Ed.; Wiley Interscience: New York, 1964. (g) Baciocchi, E. *Acc. Chem. Res.* **1979**, *12*, 430. (h) Cordes, E. H.; Jencks, W. P. *J. Am. Chem. Soc.* **1963**, *85*, 2843. (i) Banthorpe, D. V. In *Reaction Mechanism in Organic Chemistry*, Vol. 2, *Elimination Reactions*; Hughes, E. D., Ed.; Elsevier: London, 1963. (j) Beltrame, P.; Biale, G.; Lloyd, D. J.; Parker, A. J.; Ruane, M.; Winstein, S. *J. Am. Chem. Soc.* **1972**, *94*, 2240. (k) Parker, A. J.; Ruane, M.; Palmer, D. A.; Winstein, S. *J. Am. Chem. Soc.* **1972**, *94*, 2228. (l) Sicher, J. *Angew. Chem., Int. Ed. Engl.* **1972**, *11*, 200. (m) Wolfe, S. *Acc. Chem. Res.* **1972**, *5*, 102.

(2) (a) Bunnett, J. F. *Angew. Chem., Int. Ed. Engl.* **1962**, *1*, 225. (b) Bartsch, R. A.; Bunnett, J. F. *J. Am. Chem. Soc.* **1968**, *90*, 408. (c) Cram, D. J.; Greene, F. D.; DePuy, C. H. *J. Am. Chem. Soc.* **1956**, *78*, 790.

(3) DePuy, C. H.; Thurn, R. D.; Morris, G. F. *J. Am. Chem. Soc.* **1962**, *84*, 1314.

(4) For S_N2 reactions, see: (a) Bunton, C. A. *Nucleophilic Substitution at a Saturated Carbon Atom*; Elsevier: Amsterdam, 1963. (b) Ingold, C. K. *Structure and Mechanism in Organic Chemistry*, Cornell University Press: Ithaca, NY, 1969. (c) Harris, J. M. *Prog. Phys. Org. Chem.* **1974**, *11*, 89. (d) Bentley, T. W.; Schleyer, P. v. R. *Adv. Phys. Org. Chem.* **1977**, *14*, 1. (e) Parker, A. J. *Chem. Rev.* **1969**, *69*, 1. (f) Pearson, R. G.; Sobel, H.; Songstad, J. *J. Am. Chem. Soc.* **1968**, *90*, 319. (g) Lowry, T. H.; Richardson, K. S. *Mechanism and Theory in Organic Chemistry*, Harper & Row: New York, 1987.